CHEMISTRY OF MATERIALS

Article

pubs.acs.org/cm

Structural, Spectroscopic (NMR, IR, and Raman), and DFT Investigation of the Self-Assembled Nanostructure of Pravastatin-LDH (Layered Double Hydroxides) Systems

Vanessa R. R. Cunha,[†] Philippe A. D. Petersen,[‡] Marcos B. Gonçalves,[‡] Helena M. Petrilli,[‡] Christine Taviot-Gueho,[§,∥] Fabrice Leroux,[§,∥] Marcia L. A. Temperini,[†] and Vera R. L. Constantino*[,†]

[†]Departamento de Química Fundamental, Instituto de Química, Universidade de São Paulo, C. P. 26077, CEP 05513-970, São Paulo - SP, Brazil

[‡]Departamento de Física de Materiais e Mecânica, Instituto de Física, Universidade de São Paulo, C. P. 66318, CEP 05315-970, São Paulo - SP, Brazil

[§]Clermont Université, Université Blaise Pascal, Institut de Chimie de Clermont-Ferrand, BP 10448, F-63000 Clermont-Ferrand, France

[∥]CNRS, UMR 6296, ICCF, BP 80026, F-63171 Aubière, France

Supporting Information

ABSTRACT: Layered double hydroxide (LDH) nanocontainers, suitable as carriers for anionic drugs, were intercalated with Pravastatin drug using magnesium–aluminum and zinc–aluminum in a M^{II}/Al molar ratio equal 2 and different Al^{3+}/Pravastatin molar ratios. Postsynthesis treatments were used in order to increase the materials crystallinity. Hybrid materials were characterized by a set of physical chemical techniques: chemical elemental analysis, X-ray diffraction (XRD), mass coupled thermal analyses, vibrational infrared and Raman spectroscopies, and solid-state ^{13}C nuclear magnetic resonance (NMR). Results were interpreted in light of computational density functional theory (DFT) calculations performed for Sodium Pravastatin in order to assign the data obtained for the LDH intercalated materials. XRD peaks of LDH-Pravastatin material and the one-dimensional (1D) electron density map pointed out to a bilayer arrangement of Pravastatin in the interlayer region, where its associated carboxylate and vicinal hydroxyl groups are close to the positive LDH. The structural organization observed for the stacked assembly containing the unsymmetrical and bulky monoanion Pravastatin and LDH seems to be promoted by a self-assembling process, in which local interactions are maximized and chloride ion cointercalation is required. It is observed a high similarity among vibrational and ^{13}C NMR spectra of Na-Pravastatin and LDH-Pravastatin materials. Those features indicate that the intercalation preserves the drug structural integrity. Spectroscopic techniques corroborate the nature of the guest species and their arrangement between the inorganic layers. Changes related to carboxylate, alcohol, and olefinic moieties are observed in both vibrational Raman and ^{13}C NMR spectra after the drug intercalation. Thus, Pravastatin ions are forced to be arranged as head to tail through intermolecular hydrogen bonding between adjacent organic species. The thermal decomposition profile of the hybrid samples is distinct of that one observed for Na-Pravastatin salt, however, with no visible increase in the thermal behavior when the organic anion is sequestrated within LDH gap.

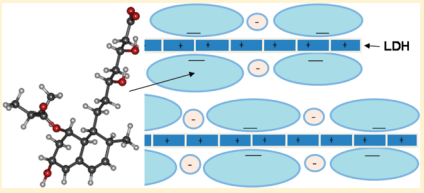

KEYWORDS: *sodium Pravastatin, X-ray diffractometry, FTIR spectroscopy, Raman spectroscopy, thermal analysis, ^{13}C NMR spectroscopy, DFT calculation*

INTRODUCTION

Layered double hydroxides (LDH) intercalated with bioactive species are promising systems for the biomedical area because of some special properties of these inorganic matrices such as high biocompatibility, low cytotoxicity, high capacity of anion loading, and possibility of surface functionalization.[1] Besides, LDH can promote the (photo)chemical and thermal stabilization of intercalated ions, increasing the shelf life of therapeutic species, and also play a role as a carrier for controlled delivery and/or site-specific release of intercalated species as drugs (anti-inflammatory, antibiotic, anticancer and antimicrobial, for example) and deoxyribonucleic acid (DNA) for gene therapy.[2] The hybrid inorganic–organic materials based on LDH present an appropriate equilibrium between chemical stability and biodegradability, permitting the release of pharmaceutical species in the organism by an ion exchange topotactic mechanism and/or by the inorganic framework dissolution.

LDH comprise positively charged layers and intercalated anions in order to keep the materials electroneutrality.[3−6] Their

Received: September 30, 2011
Revised: February 27, 2012
Published: March 9, 2012

general chemical formula is $[M^{II}_{1-x}M^{III}_{x}(OH)_2]^{x+}[A_{x/n}]^{x-}$ mH_2O, where M^{II} and M^{III} are divalent and trivalent cations and A is an exchangeable anion with charge *n*. The metal cations fill octahedral sites having hydroxide ions in the vertices. These octahedra are joined by the edges producing a large sheet. The material having magnesium and aluminum in the layers composition and carbonate ion as counterion is commercialized as an antacid. The immobilization or encapsulation of pharmaceutical substances into porous ceramic/inorganic particles is a well explored strategy to protect them for degradation in the physiological media as well as lowering the active substance concentration by a better targeting/releasing effect thus decreasing their toxicity.[7] Acting as inorganic nanocontainers, 2D materials like LDH can be engineered to achieve this purpose improving the therapeutic efficiency of many bioactive species.

Statins are a class of drugs used to reduce the cholesterol (hypercholesterolaemia) in the bloodstream and prevent cardiovascular diseases.[8] These substances inhibit the 3-hydroxy-3-methylglutaryl coenzyme A (HMGCoA) reductase, hindering the cholesterol biosynthesis and contributing to the health of arterial wall through cholesterol-independent processes. Several studies have demonstrated that cardiovascular benefices of statins are related to their anti-inflammatory properties, which open the opportunity to evaluate these drugs for the treatment of chronic disorders like rheumatoid arthritis, Parkinson's and Alzheimer's diseases.[9] Studies have also shown the potentiality of statins as anticancer drugs.[9a] The identification of other statins biological activities beyond their lipid-lowering properties deserves a more careful inspection of their physical chemistry properties in the organism. Pravastatin (3,5-dihydroxy-7- [6-hydroxy-2-methyl-8-(2-methylbutanoyloxy)-1,2,6,7,8,8a-hexahydronaphthalen-1-yl]-heptanoic acid) is a natural hydrophilic statin obtained by a two-step fermentation process, and available on the market in the sodium salt form (Figure 1) for oral administration.[10,8c]

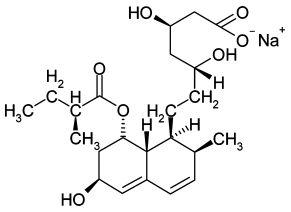

Figure 1. Schematic representation of sodium Pravastatin.

According to some reports,[11,12] sodium Pravastatin is sensitive to heat, light, and moisture, and undergoes chemical degradation in media like the stomach, which reduce its bioavailability. Hence, same patents have claimed that Pravastatin pharmaceutical formulations containing excipients with base properties like metal hydroxides can improve the drug stability.[12] The oral absorption of Pravastatin is low (34%) and occurs mainly in the intestine and to a smaller extent in the stomach.[13] The primarily general unpleasant symptoms associated with Pravastatin are constipation, flatulence, and abdominal pain.[13] Furthermore, the maximum amount of Pravastatin in the plasma occurs after a short time (1 h) and the high dose usage (to obtain the therapeutic efficacy) can lead to side effects related to the liver problems. Hence, a carrier usage can be an innovative strategy to optimize the potential of the drug in order to increase its stability in stomach and oral bioavailability. In addition, host layers can promote a decrease in the administrated dosage of the drug and keep it in an ideal level in bloodstream to ensure the treatment effectiveness. Drug delivery systems based on organic polymers,[14] receptor-targeted polymer vesicles,[15] liposomes,[16] and erythrocytes[17] have been reported in the recent literature. Considering that LDH nanocontainers are suitable carriers for anionic drugs as well as showing antacid property, a system based on Pravastatin intercalated into LDH is very interesting from a pharmaceutical point of view.

In this way, Panda et al.[18] have performed the intercalation of two statin molecules (Fluvastatin and Pravastatin) into LDH of magnesium and aluminum (Mg/Al molar ratio equal 2) by the coprecipitation method; they obtained an interlayer space of 10.1 Å for the material containing Pravastatin, which was attributed to a monolayer arrangement of the anionic drugs between the LDH layers. The authors have evaluated the *in vitro* release of the LDH-confined statins in physiological media over time and used dissolution-diffusion kinetic models to describe the intercalated drugs delivery. Both samples have showed a sustained anion release profile, a promising result in view of the oral administration of statins.

Considering the beneficial pharmaceutical properties of Pravastatin as a cholesterol-lowering drug and its pleiotropic effects, some structural and spectroscopic aspects of the LDH-Pravastatin materials deserve to be investigated in details. In this work, several synthetic parameters and characterization techniques were employed to evaluate the structure of LDH-Pravastatin materials. Syntheses of the hybrid inorganic–organic samples were carried out using magnesium–aluminum and zinc–aluminum in a M^{II}/Al molar ratio equal 2 and different Al^{3+}/Pravastatin molar ratios. Postsynthesis treatments were used in order to increase the materials crystallinity. Hybrid materials were characterized by a set of physical chemical techniques: chemical elemental analysis, X-ray diffraction, mass coupled thermal analyses, vibrational infrared and Raman spectroscopies, and solid state ^{13}C nuclear magnetic resonance (NMR). Differently of Panda et al. data,[18] the Pravastatin anion is intercalated in a bilayer fashion between the layers in the hybrid materials isolated in this work.

The characterization data are supported by computational calculations. One-dimensional (1D) electron density map was calculated from the intensity of X-ray diffraction peaks of LDH-Pravastatin material containing zinc–aluminum. Vibrational (infrared and Raman) and ^{13}C NMR spectra of sodium Pravastatin were simulated by density functional theory (DFT) in order to assign the data obtained for the LDH intercalated hybrid materials.

■ MATERIALS AND METHODS

Sodium Pravastatin ($NaC_{23}H_{35}O_7$, Henrifarma), magnesium chloride hexahydrate ($MgCl_2{\cdot}6H_2O$, Synth), aluminum chloride hexahydrate ($AlCl_3{\cdot}6H_2O$, Aldrich), zinc chloride ($ZnCl_2$, Aldrich), and sodium hydroxide (NaOH, Merck) were used without further purification.

Preparation of LDH-Pravastatin Materials. The intercalation of Pravastatin ion (abbreviated Prav) into LDH (Mg/Al or Zn/Al) host materials was performed by the coprecipitation method, as described before for LDH samples containing simple anions.[19] First, the pH of the 0.1 mol/L aqueous solution of sodium Pravastatin was adjusted to 10 by addition of a 0.2 mol/L solution of NaOH. Then, a mixed 0.1 mol/L solution of the di- and trivalent metal cations (M^{2+}/M^{3+} molar ratio equal to 2) was slowly added to the drug solution (Prav/Al^{3+}molar ratio equal to 1). The addition was made under nitrogen atmosphere with vigorous stirring until a final pH of 10. Therefore, the

dx.doi.org/10.1021/cm202953y | *Chem. Mater.* 2012, 24, 1415–1425

obtained suspension was divided into four fractions for postsynthesis treatment. The first fraction was aged at 25 °C for 1 h under a N_2 atmosphere. The other fractions were treated for 1 h at 50 °C under N_2 atmosphere as follow: heating at reflux system (abbreviated Refl), heating in a Discover microwave reactor, 50 W, (abbreviated Micro) and also in a Parr, model 4560, hydrothermal reactor (abbreviated Hydro). After each postsynthesis treatment, the suspensions were washed with deionized water by filtration under reduced pressure and the isolated solids were dried at room temperature for 48 h under reduced pressure. For the Mg_2Al-LDH composition, hybrid materials were also prepared using the molar ratios Prav/Al^{3+} equal to 2 and 3, i.e., in excess of 2 and 3 over the anion exchange capacity . In the following, the synthesized materials were abbreviated $M_2AlyPrav$, where M corresponds to the divalent metal (Mg or Zn) and y indicates the molar ratio Prav/Al^{3+} employed in the experimental preparation. The presence of chloride ions in isolated materials was verified by reaction with silver ions as follow: approximately 3 mg of LDH-Pravastatin sample was mixed with 3 mL of 0.1 mol/L nitric acid solution. After the solid solubilization, it was added about 1 mg of $AgNO_3$ in order to monitor the formation of AgCl precipitate.

Physical Measurements. Elemental chemical analyses (C, H, and N) were performed in a Perkin-Elmer model 2400 analyzer and the metal contents were determined in duplicate by ICP emission spectroscopy on an equipment Spectro Analytical Instruments at the Instituto de Química (Universidade de São Paulo-USP). X-ray diffraction (XRD) patterns of powdered samples were recorded on a Rigaku diffractometer, model Miniflex, using CuKα_1/Kα_2 radiation (1.5418 Å, 30 kV, 15 mA, scan range 1.5−70°/2θ, scan step of 0.03°/2θ and scan speed of 2°/min) and Ni filter. Mass coupled thermal analyses (TGA-DSC-MS) were recorded on a Netzsch thermoanalyser model TGA/DSC 490 PC Luxx coupled to an Aëolos 403 C mass spectrometer, using a heating rate of 10 °C/min and under synthetic air flow of 50 mL/min. Fourier transform infrared (FT-IR) spectra of samples diluted in KBr were recorded in the 4000−400 cm^{-1} range on a Bomen spectrophotometer, model MB-102, with a coupled diffuse reflectance accessory (Pike Technologies, Inc.). Fourier transform Raman (FT-Raman) spectra were recorded in a FT-Raman Bruker FRS-100/S spectrometer using 1064 nm exciting radiation (Nd:YAG laser Coherent Compass 1064−500 N) and a Ge detector. Laser power was kept below 20 mW to avoid sample degradation. ^{13}C (I = 1/2) solid state NMR experiments were performed with a 300 Bruker spectrometer at 75.47 MHz. The experiments were carried out using magic angle spinning (MAS) condition at 10 kHz and a 4 mm diameter size zirconia rotor. ^{13}C spectra obtained by proton enhanced cross-polarization method (CP, contact time of 1 ms, recycling time of 5 s) are referenced to the carbonyl of glycine calibrated at 176.03 ppm. 2000 and 10 000 scans were necessary to obtain a proper signal for sodium Pravastatin and its LDH Mg_2Al derivative, respectively.

Computational Methods. The electron density maps were obtained according to the literature[20]

$$\rho(z) = \sum_{i=0}^{\infty} F_{00l}\cos\left(\frac{2\pi lz}{c}\right)$$

where c is the unit cell parameter, z the fractional coordinate along the c stacking axis, and F_{00l} the structure factors of the 00l reflections. Nine isolated 00l reflections were used for calculating the electron density distribution of $Zn_2Al1Prav$ along the stacking axis c. F_{00l} were derived from their intensities corrected for Lorentz-polarization effects. The signs of the structure factors were directly obtained from the scattering contributions of Zn_2Al hydroxide layers, assuming a relatively small contribution of the intercalated molecules.

Density functional theory (DFT) calculations were performed using the B3LYP exchange correlation functional,[21] implemented in the Gaussian03 package.[22] The sodium Pravastatin geometry optimization using different basis sets was calculated considering the single crystal X-ray diffraction data of *tert*-octylamonium salt of Pravastatin (see Figure S1 in the Supporting Information), reported by Sato and Furukawa.[23] The Pravastatin bond distances and angles were not very sensitive to the basis set used. By applying the 6-31G** basis, the electronic structure, geometry, vibrational spectra and ^{13}C NMR isotropic chemical shifts for Sodium Pravastatin in vacuum were calculated. Tetramethylsilane (TMS), obtained with the same basis set, was used as reference for calculating the chemical shift of ^{13}C of the sodium Pravastatin. The magnetic shielding was calculated using the gauge including atomic orbitals (GIAO) method,[24] in order to eliminate the effects of gauge origin errors.[25] According to the literature,[26] the basis set 6-31G** gives a qualitative agreement with the experimental vibrational (IR and Raman) spectra. This base describes very well the experimental vibrational spectra of sodium Pravastatin with a lower computational cost. The value 0.9614 was used as the scaling factor for harmonic vibrational frequencies for the 6-31G** basis set.[27]

RESULTS AND DISCUSSION

X-ray diffraction pattern of sodium Pravastatin shows peaks at (2θ) 3.60 (24.5 Å), 6.42 (13.7 Å), 9.78 (9.03 Å), 17.1 (5.18 Å) characteristics of polymorph D,[28] whereas the powdered $Mg_2AlyPrav$ (y = 1, 2 and 3) samples exhibit similar XRD profiles typical of layered double hydroxides (see Figure S1 in the Supporting Information). As can be seen in Table S1 in the Supporting Information, for the Mg,Al couple, the chemical compositions are all close to $[Mg_2Al(OH)_6]$-$(Prav)_{0.6}Cl_{0.4}\cdot nH_2O$ whatever the value of y used for the synthesis, whereas a higher Prav amount is intercalated in Zn_2Al-LDH. Because the Prav content in both hybrid materials is not enough to neutralize the positive LDH layers, the cointercalation of chloride anions is proposed. The presence of chloride was verified by chemical analysis (as described in experimental section). The chemical analysis confirms the presence of chloride anion in the hybrid samples by the formation of a white AgCl precipitate, and additionally no gas is released when LDH samples are acid-leached, suggesting that carbonate ions are not cointercalated with Pravastatin ions. Finally, TGA-MS data also indicate the presence of chloride ions in the synthesized samples (data not shown), whereas Raman spectra point out the absence of carbonate, as will be shown ahead.

The chemical elemental analysis data suggest that the drug content in the inorganic carrier is not increased neither by a variation of the Prav/Al^{3+} molar ratio (y = 2 and 3) nor by a postsynthesis treatment; the amount of Pravastatin in the LDH matrix being constant at about 53 wt %, as shown in Table S2 in the Supporting Information. The latter treatment does not change the material XRD pattern (see Figure S2 and Table S3 in the Supporting Information). Hence it will be discussed only the characterization results obtained for $M_2Al1Prav$ (where M = Mg^{2+} and Zn^{2+}) samples. Both hybrid samples have a high content of Pravastatin as shown in Table S2 in the Supporting Information (ca. 53 g/100 g of material).

The XRD patterns of $M_2Al1Prav$ materials and Mg_2AlCl (reference sample) are presented in Figure 2. The X-ray diffraction lines are indexed in a hexagonal unit cell with the rhombohedral symmetry $R3m$, a space group that is commonly reported for LDH system. Above 30°/ 2θ, the XRD profiles are quite similar (typical of the brucite-like layers). In the low angle 2θ region, sharp harmonic diffraction lines assigned to the (00l) reflections are observed, the positions of which depend on the interlayer distance and therefore on the interlayer content. The series of (00l) peaks is listed in Table 1. The increase of the interlayer distance from 7.8 Å in Mg_2Al−Cl to 31.3 Å in $Mg_2Al1Prav$ and 30.6 Å in $Zn_2Al1Prav$ is consistent with the intercalation of Pravastatin drug between LDH layers.

dx.doi.org/10.1021/cm202953y | *Chem. Mater.* 2012, 24, 1415−1425

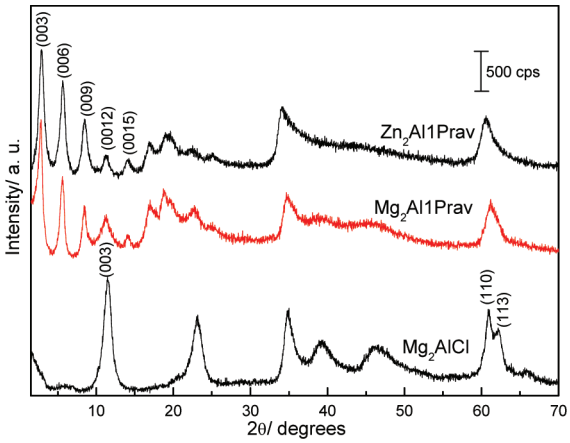

Figure 2. XRD patterns of powdered $Zn_2Al1Prav$, $Mg_2Al1Prav$, and Mg_2AlCl (from top to bottom).

Table 1. Interplanar Distances (d_{hkl}) and 2θ (λ = 1.54 Å) of LDH-Prav Samples Obtained from XRD Data

$Mg_2Al1Prav$		$Zn_2Al1Prav$		
2θ (deg)	d (Å)	2θ (deg)	d (Å)	hkl
2.82	31.3	2.88	30.6	(003)
5.61	15.7	5.64	15.7	(006)
8.40	10.5	8.46	10.4	(009)
11.3	7.82	11.2	7.90	(0012)
14.0	6.30	14.2	6.22	(0015)

The basal spacing of about 31 Å obtained in this work for the LDH-Prav materials is higher than that one observed by Panda et al.[18] for $Mg_2AlPrav$ sample (d_{003} = 15.5 Å). It is noteworthy that the first diffraction line that they observed at low 2θ angle coincides with the second diffraction lines we observe, which corresponds to the (006) reflection (Table 1); the XRD pattern showed in their paper do not display the region below 2θ about 5°. Considering the Pravastatin dimensions achieved by DFT calculation (about 10 × 10 × 7 Å, as it can be viewed in Figure S3 in the Supporting Information), it is proposed a bilayer arrangement of the organic anion in the interlayer region, with the carboxylate and hydroxyl groups close to the positive LDH layers, instead of the monolayer arrangement, as suggested before by Panda et al. The relatively fair crystallinity of $Zn_2Al1Prav$ sample allowed a profile matching refinement of the XRD pattern using FULLPROF SUITE-2000 software program (Figure 3). The intensity of the Bragg reflections thus obtained was used to calculate the one-dimension electron density projected along the c-stacking axis, displayed in Figure 4. As already shown elsewhere, the 1D plot can be used to underpin a structural model for the interlayer space.[29]

The disposition of Pravastatin anions in the LDH gallery deduced from the 1D plot is similar to that of its tert-octylamonium salt determined by single-crystal X-ray diffraction showed in Figure S4 in the Supporting Information.[23] To maximize local interactions, the hexahydronaphthyl rings supporting an alcohol group are close to each other establishing intermolecular hydrogen bonds, whereas the hydrocarbonated chains having a carboxylate and two hydroxyl groups (heptanoate group) interact through electrostatic and hydrogen bonds with the LDH layers. Finally, the butyrate groups can interact with neighbor organic species by van der Waals forces.

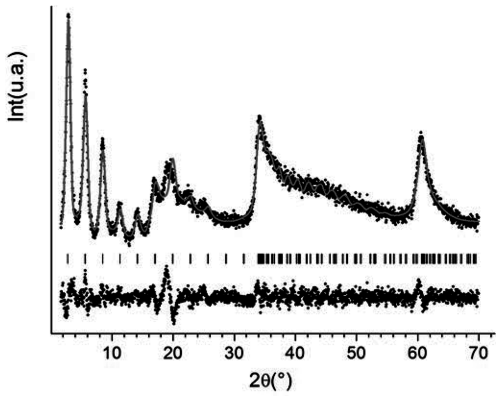

Figure 3. Profile analysis of the XRD pattern of $Zn_2Al1Prav$ sample: experimental X-ray diffraction (black dots), calculated (gray line), Bragg reflections (ticks), and difference profiles (bottom).

We believe that the dimensions of the monoanion Pravastatin, its unsymmetrical geometry and the position of the functional groups impede the fitting of its area per unit charge to that of the LDH layer and reciprocally. Therefore, it is likely that chloride anions are cointercalated to compensate the charge defect (cf. Table S1 in the Supporting Information). Indeed, the area per unit charge for M_2Al-LDH samples is about 25 Å^2, whereas Pravastatin (if represented in a rectangular parallelepiped volume with the following dimensions 10 × 10 × 7 Å) displays an area of 100 Å^2 for the base and 70 Å^2 for the area of the lateral side. In these conditions, Pravastatin anions are too large and not enough negatively charged to cover up the positive charge of LDH layers, thus not fully compensating the LDH host charge and therefore resulting in a steric constraint responsible for the incomplete intercalation of Pravastatin into M_2Al-LDH (M = Mg^{2+} or Zn^{2+}). It is worth to remember that one monovalent anion neutralizes one positive charge on one layer side; hence there is a free area on the other layer side.[30] It is well-known that Pravastatin ion has a flexible structure and different conformations are possible, what can promote a dense arrangement of the organic ions between the layers. Considering the molecular orientation deduced from the 1D plot with an area per unit charge of 70 Å^2 together with chloride anions, one may propose the interlayer arrangement as depicted in Figure 5. In this schematic representation, it is considered ten positive charges for LDH layers leading to an area of ca. 250 Å^2. The neutralization of these ten positive charges can be obtained with six Pravastatin ions in a double layer arrangement surrounded by four chloride ions (cf. Table S1 in the Supporting Information). It is quite interesting to note that the interlayer content thus estimated, i.e., "0.6 Prav, 0.4 Cl", is in good agreement with the chemical analysis. Such structural description should be understood as a straightforward self-assembling process since low mass action law (down to 1 to 1) is employed during the synthetic procedure.

TGA-DSC-MS curves of the sodium Pravastatin salt (Figure 6) show five thermal events. The first event occurs between 25 and 110 °C and is related to 1.5 wt % of water loss (DTG-MS, Figure 6b). The second event coincides with the melting point of the salt at 173 °C (endothermic process showed in Figure S4 in the Supporting Information); more exactly to the melting process of sodium Pravastatin in the polymorph D form.[28,31] The further thermal events are observed in the following temperature range (wt %): 175−290 °C (32%), 300−517 °C

dx.doi.org/10.1021/cm202953y | Chem. Mater. 2012, 24, 1415−1425

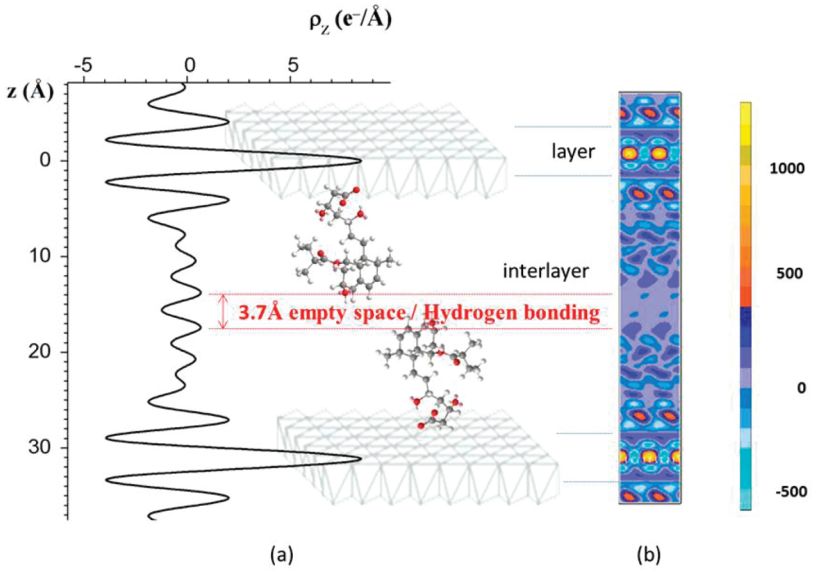

Figure 4. Schematic representation of the interlayer arrangement of Pravastatin for $Zn_2Al1Prav$: (a) One-dimension electron density projected along the *c*-stacking axis; (b) contoured Patterson map of the (x0z) plane (summed from 0 to 1 along the *b*-axis); the electron density scale is given on the right in arbitrary units.

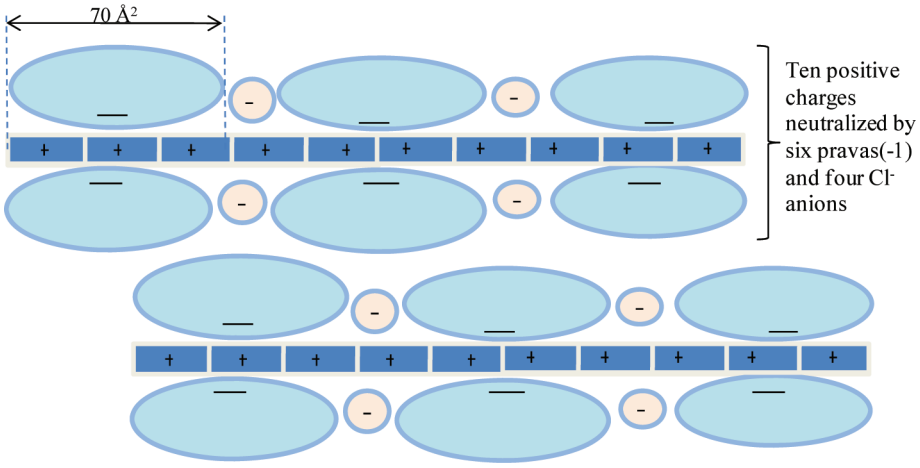

Figure 5. Schematic representation of Prav anions and chloride ions cointercalation between the positive layers of M_2Al-LDH based on area and charge calculations.

(43%), and 517−629 °C (11%). According to DTG-MS curves (Figure 6b), sodium Pravastatin is decomposed at about 175−630 °C, in air atmosphere, producing water (m/z = 18) and carbon dioxide (m/z = 44) molecules. Under the experimental conditions used in this work, no other gases were identified.

Thermal analysis data of $Mg_2Al1Prav$ and $Zn_2AlPrav$ hybrid materials are shown in Figures 7 and 8, respectively. The curves

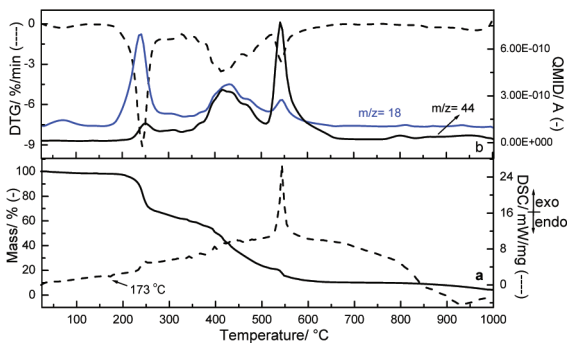

Figure 6. (a) TGA-DSC and (b) DTG-MS curves of sodium Pravastatin sample.

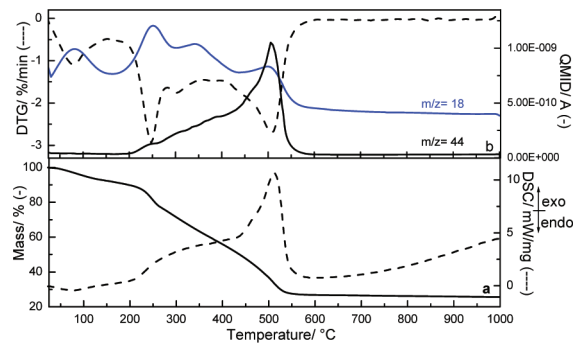

Figure 7. (a) TGA-DSC and (b) DTG-MS curves of $Mg_2Al1Prav$ sample.

dx.doi.org/10.1021/cm202953y | *Chem. Mater.* 2012, 24, 1415−1425

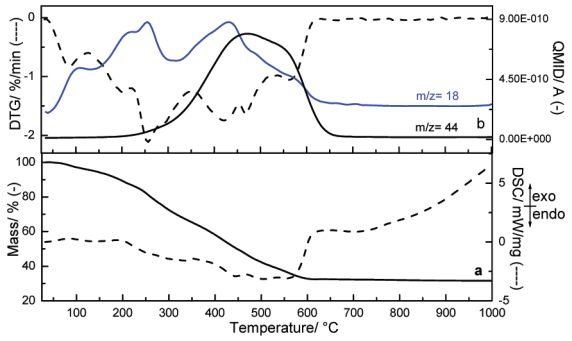

Figure 8. (a) TGA-DSC and (b) DTG-MS curves of $Zn_2Al1Prav$ sample.

reveal that the thermal stability of the confined organic species is similar to that of sodium Pravastatin with regard to the oxidative processes in air atmosphere. The first step is observed between 25 and 160 °C and gives rise to a weight loss of 8 wt % and 7 wt % for $Mg_2Al1Prav$ and $Zn_2Al1Prav$, respectively (Figures 7a and 8a). These weight losses correspond to the dehydration of both samples, as show by the DTG-MS curves (Figures 7b and 8b). In temperature range above 175 °C, the hybrid materials undergo two additional weight losses. A release of H_2O (m/z = 18) and CO_2 (m/z = 44) is observed between 177 and 460 °C (ca. 44 wt %), assigned to the simultaneous partial decomposition of LDH layers and intercalated Pravastatin. In this temperature interval, low amount of fragments associated to chlorine are also detected in the mass spectra (data not shown). The complete Pravastatin combustion and the layers dehydroxylation (exothermic process) occur between 460 - 650 °C and the event corresponds to the loss of 20 wt % and 16 wt % for $Mg_2Al1Prav$ and $Zn_2Al1Prav$, respectively. The white residues obtained at 1000 °C are 27 wt % and 32 wt % of initial mass of $Mg_2Al1Prav$ and $Zn_2Al1Prav$, respectively. Thermal analysis data show that hybrid samples have a similar thermal behavior (but distinct of the decomposition profile of Sodium Pravastatin), except that the DSC curve of $Zn_2Al1Prav$ sample does not show an exothermic event at about 500 °C.

As for the crystalline polymorphism, the molecular structure of interleaved guest is dependent on the molecular packing controlled by the intermolecular interaction but also by the host−guest charge density matching. Indeed, LDH framework is forcing the bulky Pravastatin anion to adopt a bilayer arrangement as indicated by X-ray diffraction analysis. Consequently, such accommodation may prompt the organic species to present specific interactions within the LDH inner gap, with neighbor Pravastatin ions disposed either head to tail or not.

^{13}C CPMAS NMR spectra of Pravastatin and its LDH intercalated derivative present similar feature (Figure 9). Half width of the resonance lines are somehow comparable, indicative of a similar mobility of the organic species. To scrutinize some interactions (intermolecular and with the host structure), we displayed enlarged portions from high to low field values and the chemical shifts were assigned according to the present DFT calculation and to the literature.[31,32] One can note the good agreement between the DFT calculation and the reported experimental data (Table 2). Hence, one may retrieve from 10 to 20 ppm the resonance peak of CH_3 groups (1a, 5n, 4a), then from 20 to 50 ppm, the methylene group signals 7c, 2a, 6c, 11n, 2c, 4c, the latter two being shifted due to the presence of carboxylate and hydroxyl functions, respectively. Some −CH− groups appear in that chemical shift range such as those located in the hexahydronaphthyl ring (2n, 3n, 4n) and 3a, whereas CH− directly joined to a hydroxyl function (10n, 3c, 5c) or an ester function (1n) are observed in a second enlarged portion from 60 to 80 ppm. Additional downfield shifts are observed for C═C vinyl groups (6n, 7n, 8n, 9n). Resonance peaks 6n and 8n are slightly more deshielded than 7n and 9n due to the uncompensated combination of conjugated vinyl groups deshielding 7n and 8n [respectively shielding 6n and 9n] and the $-CH(OH)$ and $-CH(CH_3)$ deshielding 9n and 6n [respectively shielding 8n and 7n], respectively. Finally the carboxyl carbons, ester (5a) and carboxylate (1c), appear in the chemical shift range 160 to 190 ppm.

As surmised by Martin-Islan et al.,[31] some Pravastatin polymorphs may differ from the coordination sphere of the carboxylate-Na^+ pair only. Indeed, the presence of a multiplets structure in the 160 to 190 ppm was attributed to several carboxylate environments since they discard the possibility of different ester carbon atoms. This case is illustrated in Figure 9 for Pravastatin salt. When incorporated into LDH gap, the carboxylate multiplet structure is suppressed and only one resonance peak located at 180.2 ppm is observed, showing that the polymorphism between D and E is absent. This may affect the CH_2 (2c) signal directly linked to the carboxylic group, located at 46.5 ppm in the salt form and screened up to 44.9 ppm for the hybrid assembly. This high-field shift for 2c indicates an electron withdrawing overall effect of the carboxylic group that may be explained by its electrostatic interaction with the LDH sheets. This interpretation will be confirmed by the Raman spectra analysis (vide infra). Additionally the peak 10n assigned to −CH−OH in the hexahydronaphthyl ring is significantly deshielded having as an effect to shift the vinyl resonance peaks; the carbons 6n and 8n, that merge together in Pravastatin salt, are split into two contributions in the hybrid material, as well as the other vicinal carbon atom 11n with a pronounced shoulder around 40 ppm. One cannot discard a shift for the other CH−OH carbons 3c and 5c as the small contribution at 74 ppm disappears and a new shoulder at 71 ppm is observed for the hybrid material. Raman spectroscopy will disentangle such combined change.

The observed modifications occurring in the 60−70 ppm and 130−140 ppm region correspond to the molecular packing and indicate some differences in the intermolecular interaction.[31] It is found here to mainly proceed through the carbon nucleus 10n bearing a hydroxyl function, this probably due to hydrogen bond interaction with a neighbor Pravastatin ion and, presumably, arranged in a head to tail fashion in the interlayer gap as illustrated from 1D projection (Figure 4). To reinforce our assumption, different environments of this hydroxyl group were found to be responsible for A and D polymorphs.[31]

To investigate the possible modifications in the Pravastatin structure when confined into LDH layers, we carried out the band assignment of sodium Pravastatin based on the literature[34] and their vibrational wavenumbers and intensities calculated by DFT method, as described in the Computational section. Figures 10 and 11 show the FT-IR and FT-Raman spectra, respectively, of the experimental and theoretical data. Despite limitations due to the fact that NaPrav spectrum was measured in the solid state whereas the calculation was performed in vacuum, a rather good agreement is observed between theoretical and experimental spectra. Table 3 presents

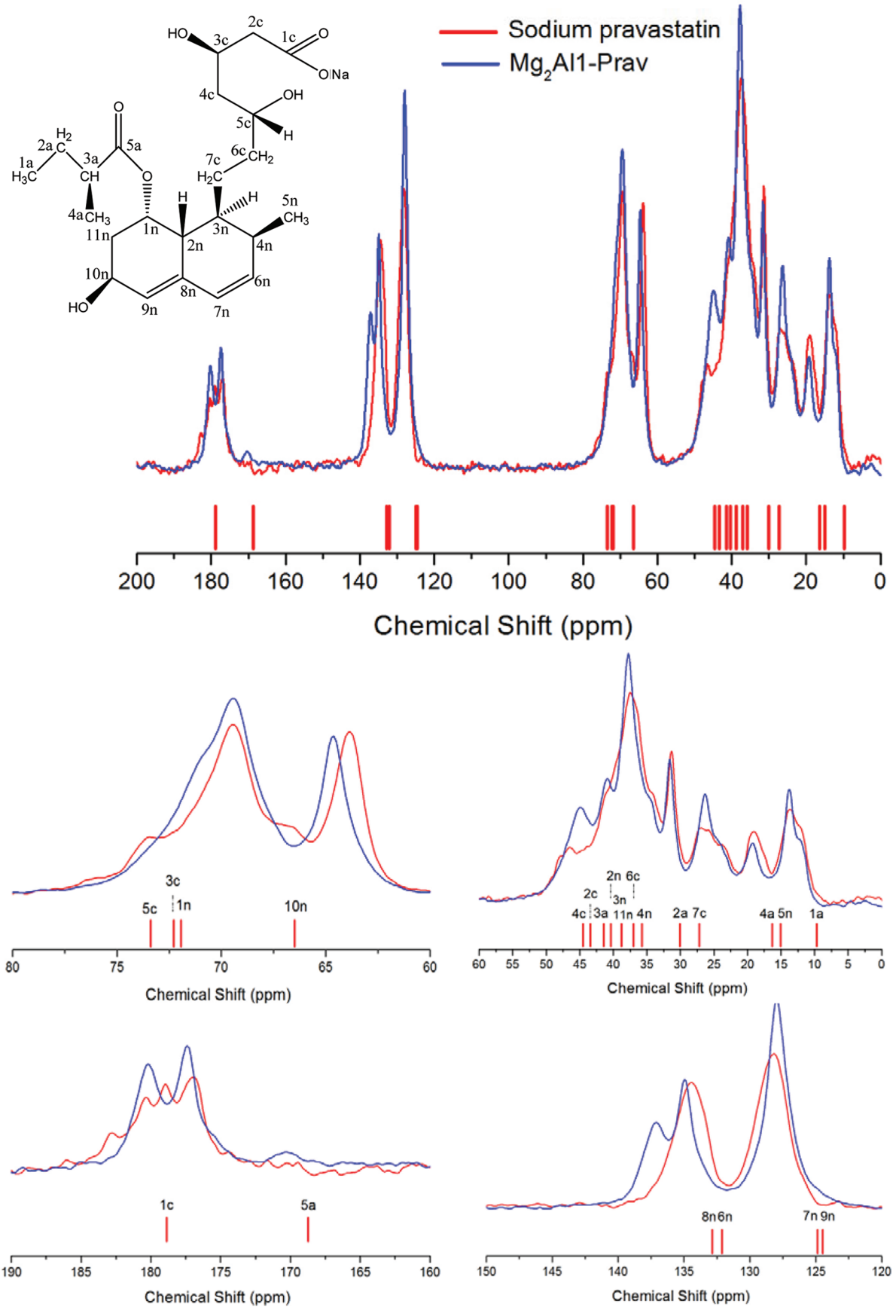

Figure 9. ^{13}C CPMAS NMR spectra of sodium Pravastatin (red line), $Mg_2Al1Prav$ (blue line) and calculated chemical shifts for sodium Pravastatin (red ticks).

dx.doi.org/10.1021/cm202953y | *Chem. Mater.* 2012, 24, 1415–1425

Table 2. Solid-State ^{13}C CPMAS NMR Chemical Shift for Sodium Pravastatin and $Mg_2Al1Prav$ Sample

	sodium Pravastatin		$Mg_2Al1Prav$	
carbon atom[a]	calcd[b]	exptl[c]	exptl	ref 32[d]
1a	9.70	12.5 (sh)	12.5 (sh)	11.70
2a	30.06	25.8/27.0	26.4	26.62
3a	41.40	41 (sh)	40.9	41.61
4a	16.32	19.0	19.3	16.74
5a	168.73	176.9/179	177.4	176.39
1n	71.94	69.46	69.48	69.20
2n	40.36	37.5	37.8	37.69
3n	38.81	36.5 (sh), 37.5	37.8	36.67
4n	35.73	31.4	31.6	31.00
5n	15.03	13.6	13.7	13.56
6n	132.13	134.4	135	135.74
7n	124.89	128.2	128	127.43
8n	132.86	134.4	137.1	135.24
9n	124.49	128.2	128	126.18
10n	66.49	63.8	64.6	64.99
11n	38.80	36.5 (sh), 37.5	37.8	36.71
1c	178.88	180.3/182.8	180.2	[e]
2c	43.42	46.5	44.9	[e]
3c	72.28	71.6 (sh)	71	62.63
4c	44.50	46.5	44.9	[e]
5c	73.38	73.6		76.05
6c	37.00	34	34.5	32.79
7c	27.20	23.6 (sh)	24 (sh)	23.77

[a]See carbon label in Figure 9. [b]Values in ppm obtained by functional/basis set BLYP/6-31G**. [c]Polymorph D. [d]Spectrum in $CDCl_3$ solution of Pravastatin in the form of lactone; [e]Lactone form.

the experimental and calculated wavenumbers of the bands and the tentative attribution considering the main groups involved in the vibration visualized by DFT method. A detailed discussion about the assignment of NaPrav can be seen in the Supporting Information.

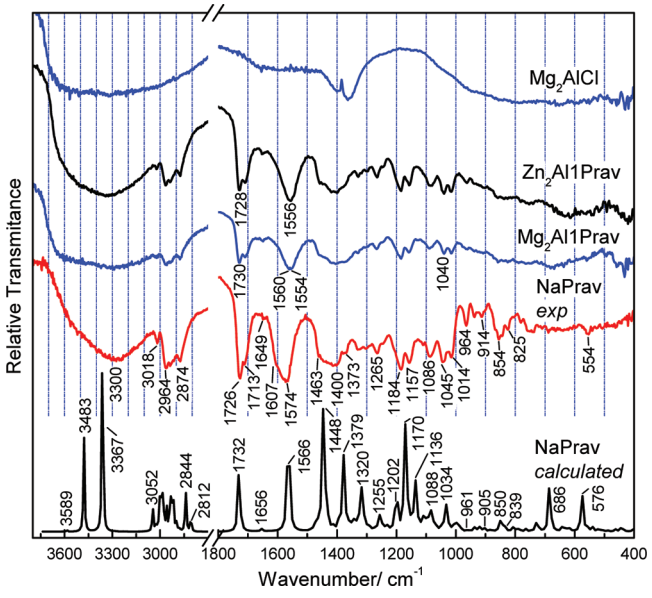

Figure 10. FT-IR spectra of calculated and experimental sodium Pravastatin, $Mg_2Al1Prav$, and $Zn_2Al1Prav$ samples. For comparison purposes, spectrum of Mg_2Al intercalated with chloride ions was inserted.

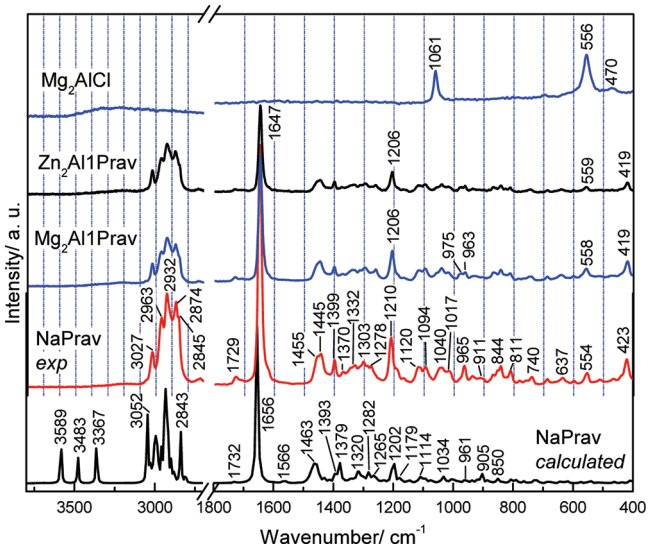

Figure 11. FT-Raman spectra of calculated and experimental Sodium Pravastatin, $Mg_2Al1Prav$, and $Zn_2Al1Prav$. For comparison purposes, spectrum of Mg_2Al intercalated with chloride ions was inserted.

Comparing the vibrational spectra of NaPrav and LDH-Pravastatin materials, a high similarity is observed, indicating that intercalation reactions preserve the drug structural integrity, as previously confirmed by ^{13}C CP MAS analysis. The FT-IR spectra of the LDH hybrid materials are dominated by a broad and intense absorption of the inorganic carrier below 1000 cm^{-1}. On the other hand, FT-Raman spectra of LDH hybrid materials are free of the water molecules and LDH hydroxide layers vibrational bands as it was reported before.[35]

The main differences between the vibrational spectra of Pravastatin in the sodium and the intercalated forms are presented ahead. The strong FT-IR absorption band at 1574 cm^{-1} is shifted to about 1560−1554 cm^{-1} ($\Delta \approx 14$−20 cm^{-1}) when the drug is intercalated, suggesting that the interaction between the LDH layers and the drug is through the carboxylate group (involving carbon 1c) and also the alcohol group (involving carbon 3c), as proposed in Figure 4. The weakening of the COO^- bonds can suggest that the LDH-Pravastatin electrostatic interaction is stronger than the Na^+-Pravastatin. ^{13}C NMR spectrum of LDH-Pravastatin (Figure 9) also shows modifications in the region related to carbons 1c and 3c. A shoulder observed at 1607 cm^{-1} decreases in intensity after the Pravastatin intercalation (this band is absent in the theoretical calculation). FT-IR spectrum of NaPrav reveals a medium band at 1045 cm^{-1} assigned to ν C−O (10n) and δ CH (cyclohexene rings) modes that it is shifted to 1040 cm^{-1} in the hybrid materials. Considering the FT-Raman spectra, other bands associated to the same groups also show modifications: the band at 1210 cm^{-1}, attributed to δ HCOH (10n) and δ =CH (olefin), is shifted to 1206 cm^{-1} after the Pravastatin confinement. Changes related to alcohol (carbon 10n at about 64 ppm) and olefinic (at about 128−135 ppm) moieties are also observed in the ^{13}C NMR spectrum after the drug intercalation. Other spectral variations confirm that olefin vibration bands are sensitive to the intercalation as illustrated by the splitting of the band at 965 cm^{-1} to 975 and 963 cm^{-1}, in the FT-Raman spectra of the hybrid materials. According to DFT calculation, this band has a great contribution of the out-of-plane deformation (δoop =CH) of hydrogen atoms linked to carbons 6n and 7n (having the hydrogen atoms out-of-phase).

dx.doi.org/10.1021/cm202953y | Chem. Mater. 2012, 24, 1415−1425

Table 3. Vibrational FT-IR and FT-Raman

sodium Pravastatin calcd[a] (cm^{-1})	sodium Pravastatin experimental[b] (cm^{-1})		$Mg_2Al1Prav$ exptl (cm^{-1})		tentative attribution[c]
	FT-IR	FT-Raman	FT-IR	FT-Raman	
3589, 3483, 3367	3300 (vb)[d]		3300 (vb)[d]		ν OH
3052, 3046, 3029	3018 (w)	3027 (13)[e]		3023	$\nu_{s,as}$ CH (olefin)
3028−2961	2964 (ms)	2963 (29)	2959	2965	ν_{as} CH (alkane)
2946−2918	2936 (ms)	2932 (39)		2930	ν_s CH (alkane)
2900, 2882	2874 (ms)	2874 (35)	2876	2876	ν CH (rings)
2843, 2844, 2812		2845 (sh)			ν CH (3c,10n,5c)[f]
1732	1726 (vs)	1729 (4)	1730	1731	ν C═O (ester)
	1713 (sh)	1706 (w)			
1656	1649 (vvw)	1647 (100)	1649 (vvw)	1648 (100)	ν_s C═C
1566	1574 (vs)		1560 (vs)		ν_{as} COO^-, δ COH (3c)
1488−1457	1463−1400 (b, vs)	1455 (14)	1463−1400 (b, vs)	1456 (sh)	δ CH (alkane), sc CH_2 (alkane)
1450−1437	1463−1400 (b, vs)	1445	1463−1400 (b, vs)	1447	δ COH (3c,5c), sc CH_2 (heptanoate)
1393	s1400 (vs)	1399 (11)	1400 (s, b)	1399 (15)	wag CH_3 (1a,5n), δ CH (6n,7n), δ COH (10n)
1379	1373 (w)	1370 (2)	1370 (s, b)	1370	ν_s COO^-, wag CH_3 (5n), wag CH_2 (4c), δ =CH (6n,7n)
1320	1331 (w)	1332 (b)	1328	1337 (b)	δ COH (3c,5c), τ CH_2 (6c), wag CH_2 (4c)
1311−1282	1310−1288 (w)	1303−1278 (4)	1310−1288 (w)		CH_2 and CH_3 deformations (heptanoate and rings)
1255	1265 (wm)		1267		δ CH (3a), τ CH_2 (2a), r CH_3 (1a)
1202	1209 (sh)	1210 (18)	1209 (sh)	1206	δ HCOH (10n), δ =CH (olefin)
1179	1184 (m)	1185 (sh)	1184	1185 (sh)	δ CH_2/ δ CH (all structure)
1170	1157 (m)	1166 (vw)	1157	1166 (vw)	ν C−O (ester), δ CH (6n,7n,3a), τ CH_2 (11n), r CH_3 (1a,4a)
1136	1134 (vvw)		1134 (vvw)		ν C−O (ester), r CH_3 (1a,4a), r CH_2 (2a)
1114	1111 (vw)	1120 (6)	1111 (vw)	1118	δ CH/ δ CH_2 (rings and heptanoate), ν CO (5c,3c)
1099		1094 (6)		1096	δ CH/ δ CH_2 (rings and heptanoate), ν CO (5c,3c)
1088	1086 (mw)		1090		δ CH/ δ CH_2 (rings and heptanoate)
1034	1045 (m)	1040 (6)	1040	1042	ν C−O (10n), δ CH (rings)
1006	1014 (m)	1017 (6)	1014	1019	δ CH (rings); wag CH_2 (2c,4c), r CH_3 (5n), ν C−C (2c,3c)
961	964 (69)	965 (6)		975, 963	δ CH_2 (heptanoate), δoop =CH (6n,7n)
905	914 (w)	911 (2)			ν C−C (1c,2c), δ COO^-
850	854 (m)	851, 844 (6)	858	844	δoop =CH (9n), δ CH_2 (2c)
839	825				ν CO (3c,5c), r CH_2 (4c)
576					δ_{oop} COH
560	554	554 (4)	554	558	δ CH/δ CH_2 (heptanoate), rings "breathing"
				558	δ HO−M−OH[d]

[a]Selected values in cm^{-1} obtained by functional/basis set B3LYP/6-31G**. The wavenumbers are shifted by 0.9614, according to the literature.[27,33] [b]Polymorph D. [c]Main groups involved in the vibration. [d]ν_s = symmetric stretching, ν_{as} = antisymmetric stretching, δ = bending, sc = scissoring, wag = wagging, r = rocking, τ = twisting, oop = out-of-plane, b = broad, vb = very broad, vs = very strong, vw = very weak; M = metals from the layer (*M* = Al^{3+}, Mg^{2+}, or Zn^{2+}). [e]Numbers in parentheses, relative intensity. [f]The numbers and letters are related to the carbon indexation in Pravastatin structure showed in Figure 9.

FT-Raman of LDH materials such as Mg_2Al intercalated with chloride ions show bands at 556 and 470 cm^{-1}, assigned to metal−OH translation modes.[36] Pravastatin also has a band at 556 cm^{-1}; hence, the bands at 558 and 559 cm^{-1} observed in the spectra of LDH-Pravastatin samples can have contributions from both the inorganic carrier and the intercalated species. It is observed a low intensity band at 1061 cm^{-1} in the Mg_2AlCl spectrum, indicating a minor contamination with carbonate ions but not significant for the LDH hybrid materials.

CONCLUSIONS

Different experimental parameters such as the molar ratio Prav/Al^{3+} and postsynthesis treatments provide Mg_2Al-Prav materials with practically the same chemical composition and crystallinity. When hybrid materials are synthesized replacing Mg^{2+} by Zn^{2+} in the intralayer region, hybrid samples exhibit higher crystallinity and Pravastatin content. From the X-ray diffraction pattern simulation of the Zn_2Al hybrid sample, a bilayer arrangement of the guest species in a head-to-tail fashion in the LDH interlayer region was proposed. Experimental and theoretical spectroscopic techniques support the orientation of Pravastatin in the inorganic matrix.

The comparison of experimental and theoretical vibrational spectroscopy shows that the main difference between sodium and intercalated forms of Pravastatin is due to the electrostatic interactions between COO^- group and the positive LDH layers as corroborated by solid-sate ^{13}C NMR data and supported by DFT simulations. Despite limitations due to the fact that NaPrav spectrum was measured in the solid state whereas the calculation was performed in vacuum, it is observed a quite agreement between theoretical and experimental spectra, allowing interpreting the experimental scenario.

dx.doi.org/10.1021/cm202953y | *Chem. Mater.* 2012, 24, 1415−1425

Interestingly, when interleaved into LDH, Pravastatin anions seem to be accommodated in a way similar to tert-octylamonium salt of Pravastatin, thus forced to be arranged as head to tail through an intermolecular hydrogen bonding interaction. This kind of organization is a consequence of Pravastatin size, asymmetry, charge and the resulting host layer charge density mismatching. The Pravastatin was also found to undergo electrostatic attractions with the inner LDH gap promoting additional interactions with its vicinal alcohol function. The structural organization observed for the system containing Pravastatin and LDH seems to be promoted by a self-assembling process, in which local interactions are maximized.

This study permitted to clarify the structure of a potential hybrid system for carrying statins like Pravastatin to the organism and to demonstrate the cointercalation of chloride anions. The presence of such easily exchangeable anion may allow to further tune the chemical composition of the LDH carrier and therefore to obtain a multifunctional action. The pleiotropic effects of this class of drugs are very important and have promoted a quite number of investigations in the health area.

■ ASSOCIATED CONTENT

Supporting Information

Listings of chemical analysis, LDH hybrid materials composition, and X-ray diffraction data. This material is available free of charge via the Internet at http://pubs.acs.org.

■ AUTHOR INFORMATION

Corresponding Author

*E-mail: vrlconst@iq.usp.br.

Notes

The authors declare no competing financial interest.

■ ACKNOWLEDGMENTS

The authors are grateful to Fundação de Amparo a Pesquisa do Estado de São Paulo (FAPESP), Conselho Nacional de Desenvolvimento Científico e Tecnológico (CNPq), Coordenação de Aperfeiçoamento de Pessoal de Nível Superior (CAPES), Comité Français dEvaluation de la Coopération Universitaire avec le Brésil (COFECUB), and Nanobiomed (Nanomedicine Network/CAPES) for financial support and scholarships. Also, the authors thank Dr. Ricardo R. F. Bento for helpful discussions about theoretical calculations.

■ REFERENCES

(1) (a) Carretero, M. I.; Pozo, M. *Appl. Clay Sci.* **2010**, *47*, 171−181. (b) Oh, J.-M.; Biswick, T. T.; Choy, J.-H. *J. Mater. Chem.* **2009**, *19*, 2553−2563.

(2) (a) Cunha, V. R. R.; Ferreira, A. M. D. C.; Constantino, V. R. L.; Tronto, J.; Valim, J. B. *Quim. Nova* **2010**, *33*, 159−171. (b) Oh, J.-M.; Choi, S.-J.; Lee, G.-E.; Han, S.-H.; Choy, J.-H. *Adv. Funct. Mater.* **2009**, *19*, 1617−1624. (c) Costantino, U.; Nocchetti, M.; Sisani, M.; Vivani, R. *Z. Kristallogr.* **2009**, *224*, 273−281. (d) Ladewig, K.; Xu, Z. P.; Lu, G. Q. *Expert Opin. Drug Deliv.* **2009**, *6*, 907−922. (e) Khan, A. I.; Ragavan, A.; Fong, B.; Markland, C.; O'Brien, M.; Dunbar, T. G.; Williams, G. R.; O'Hare, D. *Ind. Eng. Chem. Res.* **2009**, *48*, 10196−10205. (f) Desigaux, L.; Belkacem, M. B.; Richard, P.; Cellier, J.; Le'one, P.; Cario, L.; Leroux, F.; Taviot-Gueho, C.; Pitard, B. *Nano Lett.* **2006**, *6*, 199−204. (g) Leroux, F; Taviot-Gueho, C. *J. Mater. Chem.* **2005**, *15*, 3628−3642. (h) O'Hare, D. M., Drug delivery system comprising a drug intercalated between a Layered Double Hydroxide, WO 0247729, 2002; (i) Park, T.; Choy, J. H.; Oh, J. M.; Jung, J. S., Injectable drug carrier comprising Layered Double Hydroxide, WO 2006/129893, 2006.; (j) Marenzi, G.; Bolognese, A.; Califano, L.; Calignano, A.; Costantino, U.; Sammartino, G.; Vittoria, V., Controlled-delivery system of pharmacologically active substances, preparation process and medical use thereof, WO 2007/010584, 2007.

(3) Trifirò, F.; Vaccari, A. Hydrotalcite anionic clays (layered double hydroxides) In *Solid State Supramolecular Chemistry: Two and Three-Dimensional Inorganic Networks*; Alberti, G., Bein, T., Eds.; Pergamon: New York, 1996.

(4) Braterman, P. S.; Xu, Z. P.; Yarberry, F. Layered Double Hydroxides (LDHs). In *Handbook of Layered Materials*; Auerbach, S. M., Carrado, K. A., Dutta, P. K., Eds.; Marcel Dekker: New York, 2004.

(5) Cavani, F.; Trifiro, F.; Vaccari, A. *Catal. Today* **1991**, *11*, 173−301.

(6) Vaccari, A. *Catal. Today* **1998**, *41*, 53−71.

(7) Faraji, A. H.; Wipf, P. *Bioorg. Med. Chem.* **2009**, *17*, 2950−2962.

(8) (a) Davignon, J. *Circulation* **2004**, *109* (III), 39−43. (b) Corsini, A.; Bellosta, S.; Baetta, R.; Fumagalli, R.; Paoletti, R.; Bernini, F. *Pharmacol. Therapeut* **1999**, *84*, 413−428. (c) Campo, V. L.; Carvalho, I. *Quim. Nova* **2007**, *30*, 425−430.

(9) (a) Dinarello, C. A. *Cell* **2010**, *140*, 935−950. (b) Barrios-González, J.; Miranda, R. U. *Appl. Microbiol. Biotechnol.* **2010**, *85*, 869−883. (c) Tousoulis, D.; Andreou, I.; Antoniades, C.; Tentolouris, C.; Stefanadis, C. *Atherosclerosis* **2008**, *201*, 236−247. (d) Jain, M. K.; Ridker, P. M. *Nat. Rev.* **2005**, *4*, 977−987.

(10) Manzoni, M.; Rollini, M. *Appl. Microbiol. Biotechnol.* **2002**, *58*, 555−564.

(11) (a) Triscari, J.; O'Donnell, D.; Zinny, M.; Pan, H. Y. *J. Clin. Pharmacol.* **1995**, *35*, 142−144. (b) Jacobsen, W.; Kirchner, G.; Hallensleben, K.; Mancinelli, L.; Deters, M.; Hackbarth, I.; Benet, L. Z.; Sewing, K.-F.; Christians, U. *Drug Metab. Dispos.* **1999**, *27*, 173−179. (c) Hatanaka, T. *Clin. Pharmacokinet.* **2000**, *39*, 397−412.

(12) (a) Kumar, M; Talwar, N.; Raghuvanshi, R. S.; Rampal, A. K. Controlled Release Drug Delivery System of Pravastatin, U.S. Patent 2005/0089572 A1. (b) Habib, Y. S.; Ullah, I.; Jain, N. B. Enteric Coated Pravastatin Bead Formulation. WO 00/33821.

(13) Moghadasian, M. H. *Life Sci.* **1999**, *65*, 1329−1337.

(14) (a) Shidhaye, S. S.; Thakkar, P. V.; Dand, N. M.; Kadam, V. J. *AAPS PharmSciTech.* **2010**, *11*, 416−424. (b) Garg, Y.; Pathak, K. *AAPS PharmSciTech.* **2011**, *12*, 673−682.

(15) Broz, P.; Ben-Haim, N.; Grzelakowski, M.; Marsch, S.; Meier, W.; Hunziker, P. *J Cardiovasc. Pharmacol.* **2008**, *51*, 246−252.

(16) Coimbra, M; Banciu, M.; Fens, M. H. A. M.; de Smet, L.; Cabaj, M.; Metselaar, J. M.; Storm, G.; Schiffelers, R. M. *J. Controlled Release* **2010**, *148*, 303−310.

(17) Harisa, G. E. I.; Ibrahim, M. F.; Alanazi, F. K. *Int. J. Med. Sci.* **2011**, *8*, 222−230.

(18) Panda, H. S.; Srivastava, R.; Bahadur, D. *J. Phys. Chem. B* **2009**, *113*, 15090−15100.

(19) Constantino, V. R. L.; Pinnavaia, T. J. *Inorg. Chem.* **1995**, *34*, 883−892.

(20) Whittingham, M.; Jacobson, A. *Intercalation Chemistry*; Academic Press: New York, 1982.

(21) (a) Lee, C. T.; Yang, W. T.; Parr, R. G. *Phys. Rev. B* **1988**, *37*, 785−789. (b) Becke, A. D. *J. Chem. Phys.* **1996**, *104*, 1040−1046.

(22) Frisch, M. J.; Trucks, G. W.; Schlegel, H. B.; Scuseria, G. E.; Robb, M. A.; Cheeseman, J. R.; Montgomery, J. A., Jr.; Vreven, T.; Kudin, K. N.; Burant, J. C.; Millam, J. M.; Iyengar, S. S.; Tomasi, J.; Barone, V.; Mennucci, B.; Cossi, M.; Scalmani, G.; Rega, N.; Petersson, G. A.; Nakatsuji, H.; Hada, M.; Ehara, M.; Toyota, K.; Fukuda, R.; Hasegawa, J.; Ishida, M.; Nakajima, T.; Honda, Y.; Kitao, O.; Nakai, H.; Klene, M.; Li, X.; Knox, J. E.; Hratchian, H. P.; Cross, J. B.; Bakken, V.; Adamo, C.; Jaramillo, J.; Gomperts, R.; Stratmann, R. E.; Yazyev, O.; Austin, A. J.; Cammi, R.; Pomelli, C.; Ochterski, J. W.; Ayala, P. Y.; Morokuma, K.; Voth, G. A.; Salvador, P.; Dannenberg, J. J.; Zakrzewski, V. G.; Dapprich, S.; Daniels, A. D.; Strain, M. C.; Farkas, O.; Malick, D. K.; Rabuck, A. D.; Raghavachari, K.; Foresman, J. B.; Ortiz, J. V.; Cui, Q.; Baboul, A. G.; Clifford, S.; Cioslowski, J.; Stefanov, B. B.; Liu, G.; Liashenko, A.; Piskorz, P.; Komaromi, I.;

Martin, R. L.; Fox, D. J.; Keith, T.; Al-Laham, M. A.; Peng, C. Y.; Nanayakkara, A.; Challacombe, M.; Gill, P. M. W.; Johnson, B.; Chen, W.; Wong, M. W.; Gonzalez, C.; Pople, J. A. *Gaussian 03*, Revision A.1, Gaussian Inc.: Wallingford, CT, 2003.
(23) Sato, S.; Furukawa, Y. *J. Antibiot.* **1988**, *41*, 1265−1267.
(24) (a) Wolinski, K.; Hilton, J. F.; Pulay, P. *J. Am. Chem. Soc.* **1990**, *112*, 8251−8260. (b) Cheeseman, J. R.; Trucks, G. W.; Keith, T. A.; Frisch, M. J. *J. Chem. Phys.* **1996**, *104*, 5497−509.
(25) Casabianca, L. B.; de Dios, A. C. *J. Chem. Phys.* **2008**, *128*, 052201−10.
(26) Halls, M. D; Schlegel, H. B. *J. Chem. Phys.* **1999**, *111*, 8819−8824.
(27) Scott, A. P.; Radom, L. *J. Phys. Chem.* **1996**, *100*, 16502−16513.
(28) Keri, V.; Arvai, E. N.; Czovek, Z.; Kovacsne-Mezei, A.; Katai, I. V.; Racz, C. N. Methods of making Pravastatin sodium, Patent U.S. 2006 194984A1.
(29) (a) Bauer, J.; Behrens, P.; Speckbacher, M.; Langhlas, H. *Adv. Funct. Mater.* **2003**, *13*, 241−248. (b) Pisson, J.; Morel-Desrosiers, N.; Morel, J. P.; de Roy, A.; Leroux, F.; Taviot-Gueho, C.; Malfreyt, P. *Chem. Mater.* **2011**, *23*, 1482−1490.
(30) Costantino, U.; Coletti, N.; Nocchetti, M.; Aloisi, G. G.; Elisei, F. *Langmuir* **1999**, *15*, 4454−4460.
(31) Martín-Islán, A. P.; Cruzado, M. C.; Asensio, R.; Sainz-Díaz, C. I. *J. Phys. Chem. B* **2006**, *110*, 26148−26159.
(32) Bacher, M.; Baumann, K.; Knapp, H.; Steck, A.; Teibl, S. *Magn. Reson. Chem.* **2009**, *47*, 71−83.
(33) Andersson, M. P; Uvdal, P. *J. Phys. Chem. A* **2005**, *109*, 2937−2941.
(34) (a) Dollish, F. R.; Fateley, W. G.; Bentley, F. F. *Characteristic Raman Frequencies of Organic Compounds*; John Wiley & Sons: New York, 1974; (b) Nakamoto, K. *Infrared and Raman Spectra of Inorganic and Coordination Compounds. Part A: Theory and Applications in Inorganic Chemistry*; John Wiley & Sons: New York, 1997.
(35) (a) Gordijo, C. R.; Barbosa, C. A. S.; Ferreira, A; MD., C.; Constantino, V. R. L.; Silva, D. D. *J. Pharm. Sci.* **2005**, *94*, 1135−1148. (b) de Faria, D. L. A.; Constantino, V. R. L.; Baldwin, K. J.; Batchelder, D. N.; Pinnavaia, T. J.; Chibwe, M. *J. Raman Spectrosc.* **1998**, *29*, 103−108. (c) Pereira, D. C.; de Faria, D. L. A.; Constantino, V. R. L. *J. Brazilian Chem. Soc.* **2006**, *17*, 1651−1657.
(36) Kloprogge, J. T.; Hickey, L.; Frost, R. L. *J. Raman Spectrosc.* **2004**, *35*, 967−974.